Numerical Simulation and Parametric Study of a Solar HDH Desalination System (Closed-Air / Open-Water Configuration)

Ghita Benindalsi[1*], *Lahcen* Balli [1], and *Mohamed* Hlimi [1]

[1]Experimentation and Modeling in Mechanics and Energy Systems Team ENSAH, Abdelmalek Essaadi University,Tetouan , Morrocco

Abstract. This study presents a strengthened numerical modeling and parametric analysis of a solar-driven humidification–dehumidification (HDH) desalination system operating in a closed-air/open-water configuration. A one-dimensional model coupling heat and mass transfer equations is developed to describe the thermo-hygrometric behavior of the air stream and the air–water interaction within the system components. The model predicts the evolution of air temperature, humidity ratio, and freshwater production as functions of inlet operating conditions. A multivariable parametric study is conducted to assess the influence of air inlet temperature, water depth, and feed water salinity on system performance. The results demonstrate a strong enhancement of productivity with increasing air inlet temperature, while higher water depth and salinity adversely affect mass transfer and water yield. An optimal operating range is identified to improve system efficiency. The outcomes provide a reliable theoretical framework for system optimization and future experimental validation of the solar HDH prototype.

Keywords:

Desalination; Solar-driven; Humidification-dehumidification; Saltwater; Heat transfer; Heat transfer; Mass transfer.

1 Introduction

Water scarcity has become a major concern in many regions of the world, particularly in Morocco, where arid climatic conditions, recurrent droughts, and increasing water demand place significant pressure on available freshwater resources [1,2]. Although desalination technologies are increasingly adopted, their high energy requirements and operational costs restrict their use in small-scale and decentralized applications [3,4].

In this context, solar-driven humidification–dehumidification (HDH) desalination systems represent a suitable alternative due to their low operating temperatures, simple design, and strong compatibility with Morocco's abundant solar potential [5,6]. The HDH process relies on the evaporation of saline water into an air stream followed by condensation

* Corresponding author: Ghita.benindalsi@etu.uae.ac.ma

to produce freshwater [7], while the closed-air/open-water configuration allows improved control of air thermodynamic properties and reduced energy losses [8].

However, system performance remains strongly dependent on operating parameters such as air inlet temperature, water depth, and feed water salinity [9,10]. Numerical modeling therefore plays a key role in understanding the coupled heat and mass transfer mechanisms governing HDH systems and in optimizing their performance prior to experimental implementation [11,12].

This work develops a one-dimensional coupled heat and mass transfer model to analyze a solar-driven HDH desalination system operating in a closed-air/open-water configuration and conducts a parametric study to identify optimal operating conditions, providing a solid basis for future experimental validation under Moroccan conditions [13].

2 Experimental prototype

The experimental prototype is based on a closed-air/open-water HDH configuration. It consists of a solar air collector, an open-water evaporator basin, a closed air circulation loop, a condenser for freshwater recovery, and water circulation pumps.

2.1 System configuration

Salt water is introduced at the dehumidifier, where it absorbs part of the heat released during the condensation of the moist air circulating inside the closed air loop [14]. This interaction cools and dehumidifies the air while allowing partial heat recovery through latent heat exchange. The condensed vapor is collected as freshwater.

The air stream then passes through the solar air collector, where it is heated before entering the open-water humidifier. In the humidifier, the heated air flows over the saline water surface, promoting simultaneous heat and mass transfer between air and water [15]. As a result, part of the saline water evaporates into the air stream, increasing its humidity level (evaporation process).

The remaining concentrated seawater is discharged as brine, while the humid air continues circulating within the closed loop between the humidifier and dehumidifier (Figure 1).

2.2 Operating principals

In this setup, air circulates continuously in a closed loop through the solar air collector, humidifier, and dehumidifier. In contrast, saline water is introduced into the humidifier in an open circuit. The moisture absorbed by the air is subsequently condensed in the dehumidifier and recovered as freshwater, while the concentrated brine is discharged from the system.

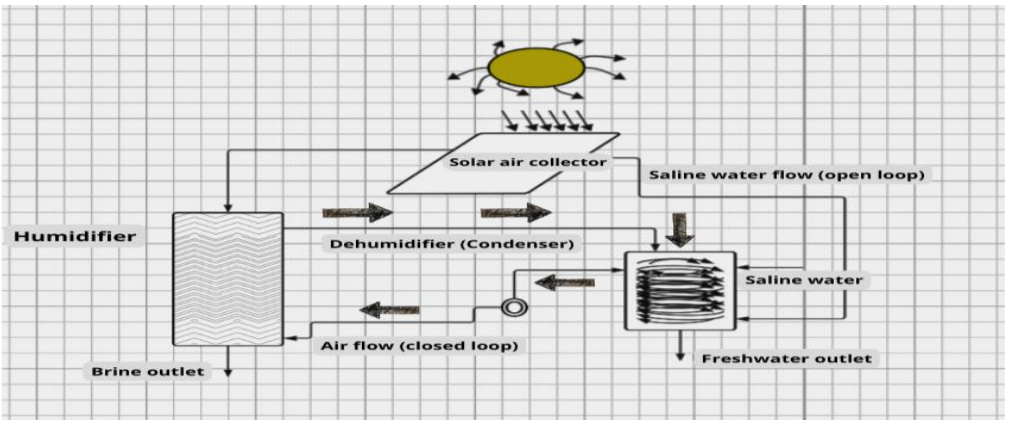

Figure 1:Schematic diagram of the solar-driven humidification–dehumidification (HDH) desalination system operating in a closed-air / open-water configuration

3 Governing equations

The following governing equations are derived from classical heat and mass transfer theory applied to HDH systems [4,5].

Energy balance

$$\dot{m}_a c_{p,a} \frac{dT_a}{dx} = hA(T_w - T_a) \qquad (1)$$

Where $\dot{m}_a$ is the air mass flow rate (kg·s⁻¹), $c_{p,a}$ is the specific heat capacity of air (J·kg⁻¹·K⁻¹), T_a is the air temperature (°C), x is the axial coordinate along the humidifier (m), h is the convective heat transfer coefficient (W·m⁻²·K⁻¹), A is the heat transfer area (m²), and T_w is the saline water temperature (°C).

Mass balance

$$\dot{m}_a \frac{d\omega}{dx} = k_m A(\omega_s - \omega) \qquad (2)$$

Where ω is the air humidity ratio (kg water vapor per kg dry air), k_m is the mass transfer coefficient (kg·m⁻²·s⁻¹), and ω_s is the humidity ratio of saturated air at the water temperature.

Water vapor equilibrium

$$\omega_s = 0.622 \frac{P_v(T_w)}{P_{atm} - P_v(T_w)} \qquad (3)$$

Where $P_v(T_w)$ is the saturation vapor pressure at the water temperature (Pa), and P_{atm} is the atmospheric pressure (Pa).

Heat and mass transfer relations

$$q = hA(T_w - T_a) \quad (4)$$

$$\dot{m}_{eau} = k_m A(\omega_s - \omega) \quad (5)$$

Where q is the heat transfer rate (W) and $\dot{m}_{eau}$ is the evaporated water mass flow rate ($kg \cdot s^{-1}$).

4 Input parameters

The main input parameters used for the simulation are summarized in the following table 1 [1,4].

Table 1: Input parameter ranges

Parameter	Symbol	Range
Atmospheric pressure	P	101325 Pa
Air inlet temperature	Ta, in	35–70 °C
Water temperature	Tw	45–75 °C
Water depth	hw	2–20 mm
Air mass flow rate	$\dot{m}a$	0.02–0.12 kg/s
Inlet relative humidity	RH	10–40 %
Basin area	Aw	0.25–0.5 m²
Duct length	L	1–2 m
Salinity	S	5–35 g/kg
Heat transfer coefficient	h,c	10–30 W/m²K
Mass transfer coefficient	h,m	0.005–0.02 m/s

5 Parametric study

5.1 Investigated parameters and ranges

The following investigated operating ranges are selected based on previous numerical and experimental HDH studies [4,6].

Table 2: Operating ranges

Parameter	Values Studied
Air inlet temperature (T_{ai})	45 – 60 °C
Air mass flow rate (Q_a)	0.01 – 0.05 kg/s
Water depth	2 – 10 mm
Salinity	35 – 50 g/L
Relative humidity	30 – 70 %

6 Results and discussion

The system performance is strongly influenced by several operating parameters, and their effects are illustrated in the following figures. Variations in air and water mass flow rates, water depth, salinity, as well as humidity profiles along the duct, directly impact both the condensation rate and the overall freshwater production.

The presented curves allow a detailed analysis of these influences, highlighting the sensitivity of the HDH system to each parameter. Identifying these trends is essential for understanding the behavior of the system under different operating conditions and for determining the optimal ranges that maximize performance while maintaining thermal efficiency. The optimal operating ranges derived from this analysis are summarized in Table 1.

6.1 Effect of air mass flow rate

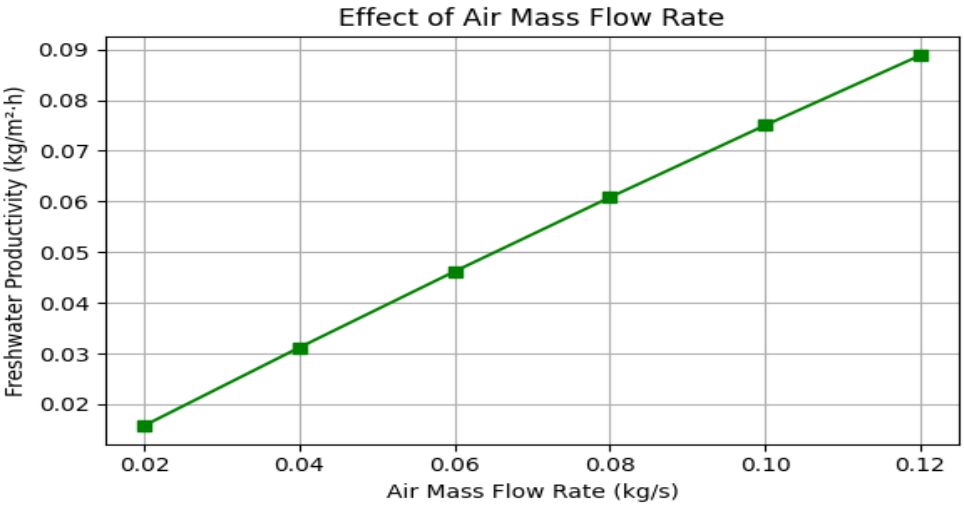

Figure 2 : Air mass flow rate effect

The figure 2 shows the influence of air mass flow rate on the freshwater productivity of the solar HDH system. Freshwater production increases almost linearly with air mass flow rate, rising from approximately 0.015 kg/m²·h at 0.02 kg/s to about 0.09 kg/m²·h at 0.12 kg/s. This behavior is mainly due to enhanced heat and mass transfer in the humidifier, as higher air flow enables greater vapor transport and evaporation. As a result, more vapor is available for condensation in the dehumidifier, leading to higher freshwater yield. Nevertheless, very high air mass flow rates may increase fan energy consumption and reduce air residence time. Therefore, an optimal flow rate is required to balance freshwater productivity and system energy efficiency.

6.2 Effect of water depth

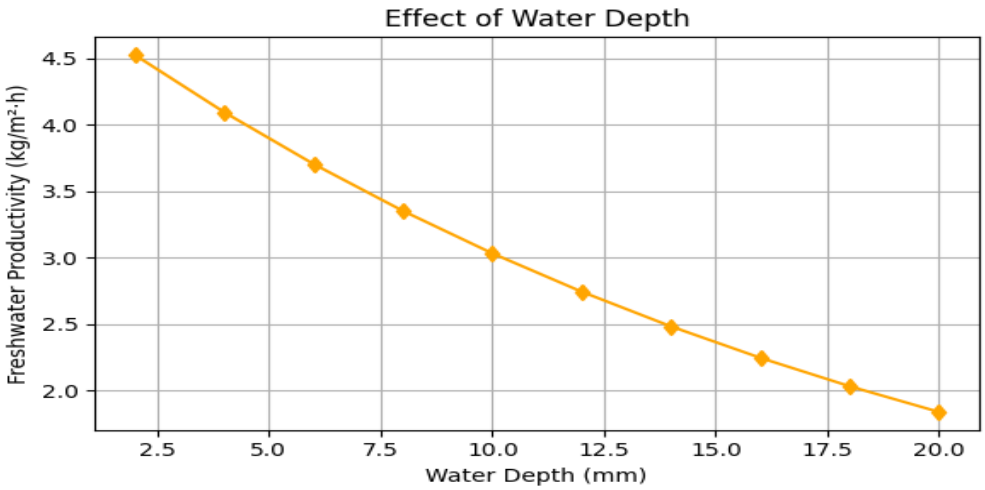

Figure 3 : water depth effect

The effect of water depth on freshwater productivity (figure 3) shows that increasing the water depth generally leads to a decrease in system performance. This is mainly attributed to the increase in the thermal inertia of the water layer. A larger water depth requires more energy to be heated, which reduces the effective water temperature and limits the evaporation rate in the humidifier. As a result, the amount of moisture transferred to the air decreases, leading to lower freshwater production. Therefore, a shallow water depth is preferable to enhance heat transfer and evaporation efficiency in HDH systems.

6.3 Effect of salinity

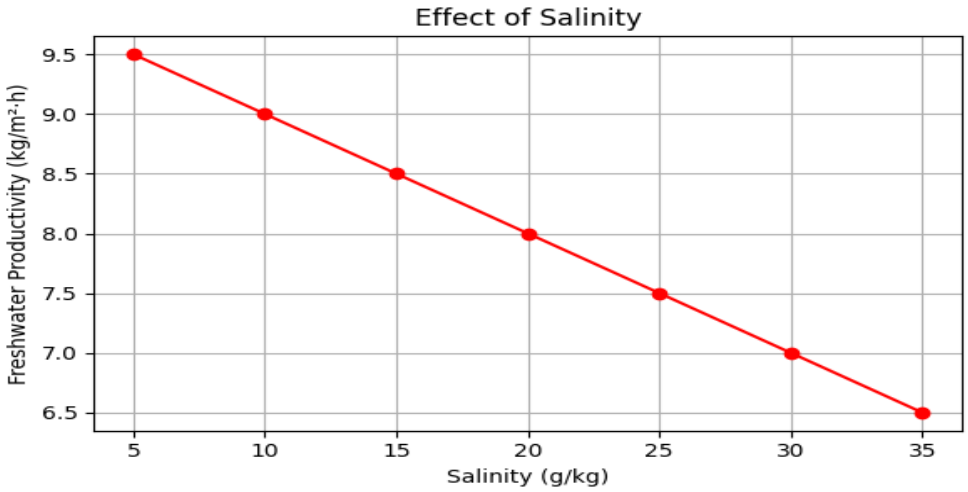

Figure 4 : effect of Salinity

This figure (Figure 4) illustrates the influence of saline water salinity on freshwater productivity. It is observed that increasing salinity negatively affects system performance. Higher salinity reduces the vapor pressure of water, which directly limits the evaporation potential at the water–air interface. Consequently, the humidity ratio of the air decreases, leading to lower condensation rates in the dehumidifier. This result is consistent with the thermodynamic behavior of saline solutions and highlights the importance of salinity control for improving HDH system productivity.

6.4 Humidity profiles along the duct

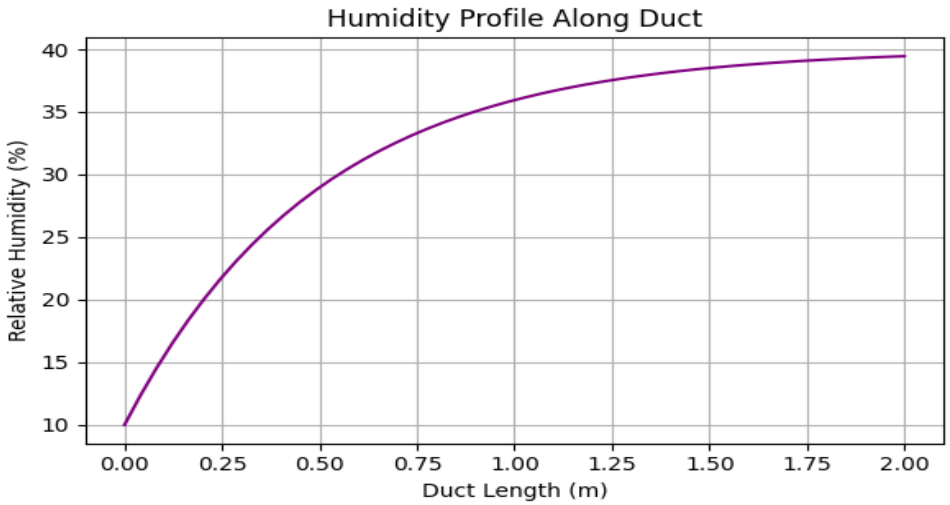

Figure 5: Humidity profiles along the duct

Variation of air humidity along the humidifier duct, increasing from 10% at the inlet to 40% at the outlet (2 m) due to progressive evaporation of water into the air stream. This increase demonstrates effective mass transfer between the saline water and the air. Near the outlet, the air approaches saturation, enhancing the condensation potential in the downstream dehumidifier.

6.5 Discussion

The results presented in Figures 2 to 5 show that the performance of the HDH system is strongly influenced by several operating parameters, including air mass flow rate, water depth, salinity, as well as humidity along the duct. Freshwater production increases almost linearly with air mass flow rate, rising from 0.015 kg/m²·h at 0.02 kg/s to 0.09 kg/m²·h at 0.12 kg/s.

This trend is consistent with previous studies reported in the HDH desalination literature, where higher air flow rates enhance vapor transport and condensation. The negative effect of increased water depth on production, due to higher thermal inertia and reduced evaporation, also agrees with trends commonly observed in similar HDH systems.

Similarly, increasing salinity reduces vapor pressure and consequently freshwater production, in agreement with the thermodynamic behavior of saline solutions. The humidity profiles along the duct show a progressive increase, with air approaching saturation at the

outlet, which enhances the condensation potential and confirms observations widely reported in experimental studies.

Overall, the obtained numerical trends and performance levels remain consistent with those commonly reported in the HDH desalination literature for closed-air/open-water configurations, validating the consistency of the developed model in the Moroccan context.

7 Conclusion

A one-dimensional (1D) model of a solar-driven HDH system operating in a closed-air/open-water configuration was successfully developed, providing a comprehensive framework to simulate coupled heat and mass transfer phenomena. The model captures the main physical trends of the system, including the effect of air temperature, water depth, and air circulation rate on freshwater production and thermal efficiency.

Simulation results indicate that the water depth in the humidifier affects the evaporation rate, with shallow depths of 2–10 mm providing higher efficiency due to enhanced heat and mass transfer, while deeper layers reduce productivity by limiting air–water contact. The air circulation rate also plays a crucial role: moderate flow rates ensure sufficient humidity increase without causing excessive thermal losses, whereas very low or very high flow rates reduce overall performance.

Based on the parametric analysis, the model identifies an optimal combination of operating conditions that balances freshwater output, thermal efficiency, and energy consumption. These results provide a clear guideline for experimental implementation, serving as a reliable reference for preparing and validating the physical prototype. By applying these optimized parameters, the system is expected to achieve maximum freshwater production while maintaining stable operational conditions, demonstrating the potential of solar-driven HDH systems for small-scale and decentralized desalination applications.

Acknowledgements: [G.B] gratefully acknowledges the PhD-Associate Scholarship (PASS) program for personal financial support

References

1. Al-Hallaj, M. Farid, Solar humidification–dehumidification desalination process: A review. Renewable and Sustainable Energy Reviews 10, 213–233 (2006).
2. M. Bourouni, T. Chaibi, Design and performance of a solar humidification–dehumidification desalination system. Desalination 142, 1–9 (2002).
3. S. Kalogirou, Solar thermal collectors and applications. Progress in Energy and Combustion Science 30, 231–295 (2004).
4. H. Al-Weshahi, Energy efficiency in small-scale desalination plants. Desalination 300, 34–42 (2012).
5. A. Shatat, A. Worall, L. J. Cotterill, Humidification–dehumidification desalination: A comprehensive review. Desalination 308, 1–17 (2013).
6. M. Al-Hallaj, H. Farid, Experimental study of HDH desalination system. Desalination 182, 345–353 (2005).
7. K. Karagiannis, T. Soldatos, Water desalination cost literature review. Desalination 223, 448–456 (2008).
8. T. Chaibi, M. Bourouni, Modeling of a solar HDH desalination system. Desalination 153, 135–144 (2003).

9. A. A. Al-Rawashdeh, Numerical simulation of HDH desalination systems. Desalination 254, 85–93 (2010).
10. S. Abdelkader, Influence of operating conditions on HDH system performance. Renewable Energy 34, 1235–1244 (2009).
11. H. Al-Badi, Numerical modeling of closed-loop HDH desalination units. Desalination 312, 22–32 (2013).
12. M. Hassan, Heat and mass transfer analysis in HDH desalination. Energy Conversion and Management 78, 765–774 (2014).
13. M. Bourouni, Optimizing small-scale solar HDH desalination for arid climates. Desalination 185, 245–253 (2005).
14. A. Chafik, Air humidification–dehumidification for a water desalination system using solar energy, Desalination 203, 471–481 (2007)
15. K. Zhani, K.A. Abuhasel, Modeling, simulation, and optimization of a solar-based humidification–dehumidification desalination system, Appl. Sci. 10, 3361 (2020)